

## ORIGINAL COMMUNICATION

# Documentation and Three-Dimensional Modelling of Human Soleus Muscle Architecture

ANNE M. AGUR,<sup>1\*</sup> VICTOR NG-THOW-HING,<sup>2</sup> KEVIN A. BALL,<sup>3</sup> EUGENE FIUME,<sup>2</sup>  
AND NANCY HUNT McKEE<sup>4</sup>

<sup>1</sup>*Division of Anatomy, Department of Surgery, University of Toronto, Toronto, Canada*

<sup>2</sup>*Department of Computer Science, University of Toronto, Toronto, Canada*

<sup>3</sup>*Faculty of Physical Education and Health, University of Toronto, Toronto, Canada*

<sup>4</sup>*Division of Plastic Surgery, Department of Surgery, University of Toronto, Toronto, Canada*

The purpose of this study was to visualize and document the architecture of the human soleus muscle throughout its entire volume. The architecture was visualized by creating a three-dimensional (3D) manipulatable computer model of an entire cadaveric soleus, in situ, using B-spline solid to display muscle fiber bundles that had been serially dissected, pinned, and digitized. A database of fiber bundle length and angle of pennation throughout the marginal, posterior, and anterior soleus was compiled. The computer model allowed documentation of the architectural parameters in 3D space, with the angle of pennation being measured relative to the tangent plane of the point of attachment of a fiber bundle. Before this study, the only architectural parameters that have been recorded have been 2D. Three-dimensional reconstruction is an exciting innovation because it makes feasible the creation of an architectural database and allows visualization of each fiber bundle in situ from any perspective. It was concluded that the architecture is non-uniform throughout the volume of soleus. Detailed architectural studies may lead to the development of muscle models that can more accurately predict interaction between muscle parts, force generation, and the effect of pathologic states on muscle function. *Clin. Anat.* 16:285–293, 2003. © 2003 Wiley-Liss, Inc.

**Key words:** anatomy; soleus; skeletal muscle; architecture; modelling

## INTRODUCTION

The architecture of a muscle consists of its external configuration and dimensions, and the internal arrangement and morphology of the contractile and connective tissue elements. Muscle fiber architecture has been documented by measuring fascicle (fiber bundle) length, angle of pennation, muscle belly length, and the volume/mass of the muscle (Yamaguchi et al., 1990). Two muscles having the same external configuration may differ in function due to differences in internal arrangement, i.e., the “design” of contractile and connective tissue elements (Lieber and Friden, 2000). Fiber length, the number of muscle fibers lying in parallel, and the angle of pennation are important in determining the amount of force a muscle is capable of producing (Woittiez et al., 1984; Enoka, 1988; Zajac, 1989).

Historically, morphologic studies of muscle have been purely descriptive in nature (Otten, 1988), but a quantitative analysis of muscle architecture is impor-

tant because the structural parameters have a profound effect on muscle function (Muhl, 1982; Woittiez et al., 1983). Architectural data form an integral part of mathematical models that have been developed to study skeletal muscle (Huijing and Woittiez,

Grant sponsors: AO/ASIF Foundation, Switzerland; Department of Surgery, University of Toronto.

Victor Ng-Thow-Hing's current address is Fundamental Research Labs-Silicon Valley, Honda R&D Americas, Inc., Mountain View, CA.

Kevin A. Ball's current address is New York Chiropractic College, Seneca Falls, NY.

\*Correspondence to: Anne M. Agur, Division of Anatomy, Department of Surgery, Medical Sciences Building Room 1158, University of Toronto, Toronto, Ontario, Canada M5S 1A8.  
E-mail: anne.agur@utoronto.ca

Received 20 March 2002; Revised 28 August 2002

Published online in Wiley InterScience (www.interscience.wiley.com). DOI 10.1002/ca.10112

TABLE 1. Summary of Mean Architectural Data of Published Cadaveric Studies of Soleus<sup>a</sup>

Author (year)	<i>n</i>	Part of soleus	FL (mm)	θ (degrees)	MT (mm)	Mass (g)	Volume (ml)	ML (mm)
Alexander and Vernon (1975)	1	—	—	20	12	264	—	—
Cutts (1988)	3	—	—	19	—	—	—	—
Friederich and Brand (1990)	2	—	30.3	32 ( <i>n</i> = 1)	—	—	374	335
Haines (1932)	1	—	34.0	—	—	—	—	—
Spoor et al. (1991)	3	Posterior	25.8	34	—	—	231	275
		Anterior	26.7	31	—	—	50	204
Trzenschik and Loetzke (1969)	5	Posterior	28.6	20	—	116.0	—	—
		Anterior	27.8	25	—	28.9	—	—
Wickiewicz et al. (1983)	2	—	19.5	25	—	215 ( <i>n</i> = 1)	—	309

<sup>a</sup>FL, fiber length; θ, angle of pennation; MT, muscle thickness; ML, muscle length.

1984; Herzog and ter Keurs, 1988; Otten, 1988; Huijing et al., 1989; Legreneur et al., 1996; Roy and Ishihara, 1997; van der Linden et al., 1998); however, human muscle architectural data are incomplete and based on relatively small sample sizes (Pierrynowski and Morrison, 1985; Yamaguchi et al., 1990). The architectural parameters of skeletal muscle have usually been defined by one average value for the entire muscle, regardless of the complexity of pennation (Wickiewicz et al., 1982; Friederich and Brand, 1990). The architectural parameters obtained from cadaveric studies of the human soleus muscle are summarized in Table 1. The experimental protocol for each study varies, making the comparison of results difficult. Furthermore, the data collection is designed to establish one average value of each of the architectural parameters for the soleus as a whole or for the anterior and posterior parts separately. Often any information gaps have been filled by estimating the parameter using anatomy atlases (Pierrynowski, 1982; Yamaguchi et al., 1990). The large number of empty spaces in Table 1 shows how few data there are quantifying the architectural parameters of the human soleus muscle. If the architectural data are scarce and do not reflect the actual structure of the component parts of a muscle, predictions based on these data only approximate reality.

The purpose of this study is to document the architecture of the human soleus muscle throughout the entire volume of the muscle. This muscle was chosen because it is functionally important and is easily accessible in the leg. The soleus is an antigravity muscle that plantar flexes the ankle. It helps keep the body erect and participates in all forms of locomotion.

## MATERIALS AND METHODS

The soleus muscle is divided into marginal, posterior, and anterior parts (Agur and McKee, 1997; Oxorn et al., 1998). The parts of soleus (Fig. 1) are defined as follows:

- Marginal soleus: Fiber bundles span from the medial, lateral, and superior margins of the posterior aponeurosis to the anterior aponeurosis medially and laterally, and the tibia and fibula superiorly. The medial and lateral fiber bundles are curved. Superiorly the fiber bundles are oriented more vertically.
- Posterior soleus: Fiber bundles attach to the posterior surface of the anterior aponeurosis and the anterior surface of the posterior aponeurosis. The fiber bundles are directed from anterosuperior to posteroinferior.
- Anterior soleus: The anterior soleus is bipennate and is best visualized on the anterior surface of the muscle. The fiber bundles join the median septum and the anterior aponeurosis. The median septum is a vertical sheet of aponeurosis. Fiber bundles of anterior soleus attach to its medial and lateral surfaces and are directed superomedially and superolaterally.

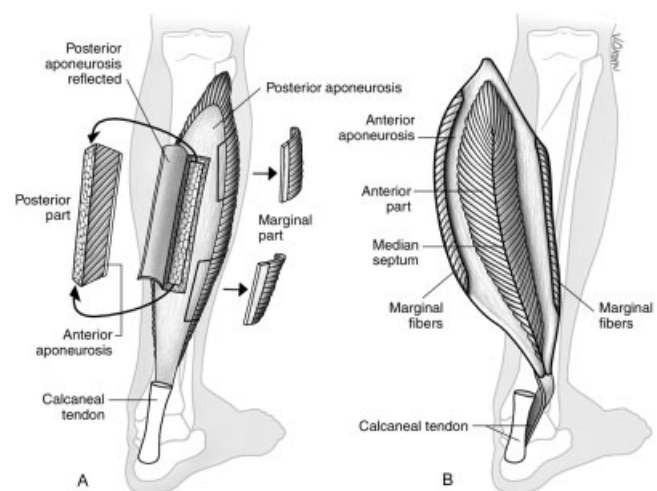


Fig. 1. Parts of the soleus muscle. **A:** Marginal and posterior soleus, posterolateral view. **B:** Anterior and marginal soleus, anterior view. Note that the soleus has been reflected from its tibial and fibular attachments and rotated.

Five formalin-fixed cadaveric soleus muscles were serially dissected *in situ*. On inspection, the cadaveric legs had no evidence of musculoskeletal deformity and the ankle joints were fixed in the anatomical position. Development of the dissection protocol continued to evolve from the first to the fifth specimen. Dissection of the fifth specimen, which was the soleus muscle of a right leg, was the most detailed and is described in this study. The method of measurement of the architectural parameters was not altered from the first to the fifth specimen. Only the dissection technique, to expose and pin increasingly more fiber bundles, evolved from the first to the fifth specimen. Data obtained from the fifth specimen was analyzed.

At each level of dissection, 50–100 fiber bundles were pinned and the specimens were photographed using three spatially calibrated cameras. The images were transferred to CD-ROM and the locations of the pins were digitized. Using direct linear transformation, the digitized 2D coordinates were used to generate 3D coordinates representing the orientation of each of the dissected fiber bundles (Ball and Pierzynowski, 1995; Agur, 2001). The 3D coordinates were fitted into DANCE, a B-spline solid model, developed by our computer science team members (Ng-Thow-Hing, 2001). The model parameterizes an enclosed volume (muscle fiber bundles) as well as its boundary surface (external surface) using 3D vector functions. Once the B-spline solid model of the soleus has been fitted with its external surface and internal volume arrangements (i.e., fiber bundles), one can generate manipulatable 3D models of the muscle to visualize its complex architecture (Agur, 2001). Plots of the muscle as a whole and of its component parts were used to observe and verify the architecture (Agur and McKee, 1997).

Using the 3D coordinates, fiber bundle length, direction, and angle of pennation were computed automatically throughout the muscle. Fiber bundle length (mm) was obtained by summing the lengths of the line segments joining sampled points of each fiber bundle (Press et al., 1992; Ng-Thow-Hing, 2001).

The point of attachment of the fiber bundle to the aponeurosis is three-dimensional and can be characterized by the position of attachment and the orientation of the fiber with respect to the surface of the aponeurosis. The angle of pennation was calculated at the attachment site at each end of the fiber bundle, as the angle between the tangent vector of the fiber bundle and the tangent plane of the muscle surface at the point where the fiber bundle meets the aponeurosis. It is important to note that previously cited data in the literature have been measured in 2D using a

protractor, caliper, or ruler. In effect, only a planar component of the true force vector was captured.

The mean, standard deviation, and range of fiber length and angle(s) of pennation were calculated for the following regions of soleus:

- the medial and lateral fiber bundles of the proximal, middle, and distal thirds of the marginal soleus;
- the medial, middle, and lateral fiber bundles of the proximal, middle, and distal thirds of the posterior soleus; and
- the medial and lateral fiber bundles of the tip and proximal, middle, and distal thirds of the anterior soleus.

For the marginal and posterior soleus, a total of 100 fiber bundles (streamlines) were measured. In the anterior soleus, 50 fiber bundles in each of the four layers were documented.

## RESULTS

### 3D Visualization of Soleus Muscle Architecture

The computer model allowed full reconstruction of all parts of the soleus muscle from the digitized data. The 3D model is fully manipulatable allowing visualization of the muscle fiber bundles from any angle. The fiber bundles are displayed throughout the volume of the muscle (Fig. 2) and can be animated to show sequential arrangement of fiber bundles (Fig. 3).

The computer model contains a B-spline solid that has been built using a continuous volume sample function (Ng-Thow-Hing, 2001). The B-spline solid can capture detailed muscle architecture in 3D. Once the original digitized data has been entered into the model, additional fiber bundles (streamlines) can be generated. Because the streamlines have an analytical expression, the physical dimensions of the new fiber bundles can be computed, added to the B-spline solid, and visualized. We designed fiber generation techniques based on Sobol sequences (Ng-Thow-Hing, 2001) to evenly distribute the fibers throughout the volume of the muscle.

Still frames from the computer program have been reproduced in black and white from a variety of views for the marginal, posterior, and anterior soleus of the right leg (Fig. 2). Each figure includes the original data set (template) and loosely and densely packed fiber bundles (streamlines). Figure 4 shows the entire soleus with all three parts assembled.

The fiber bundles of marginal soleus are curved and directed anterosuperiorly along the medial and

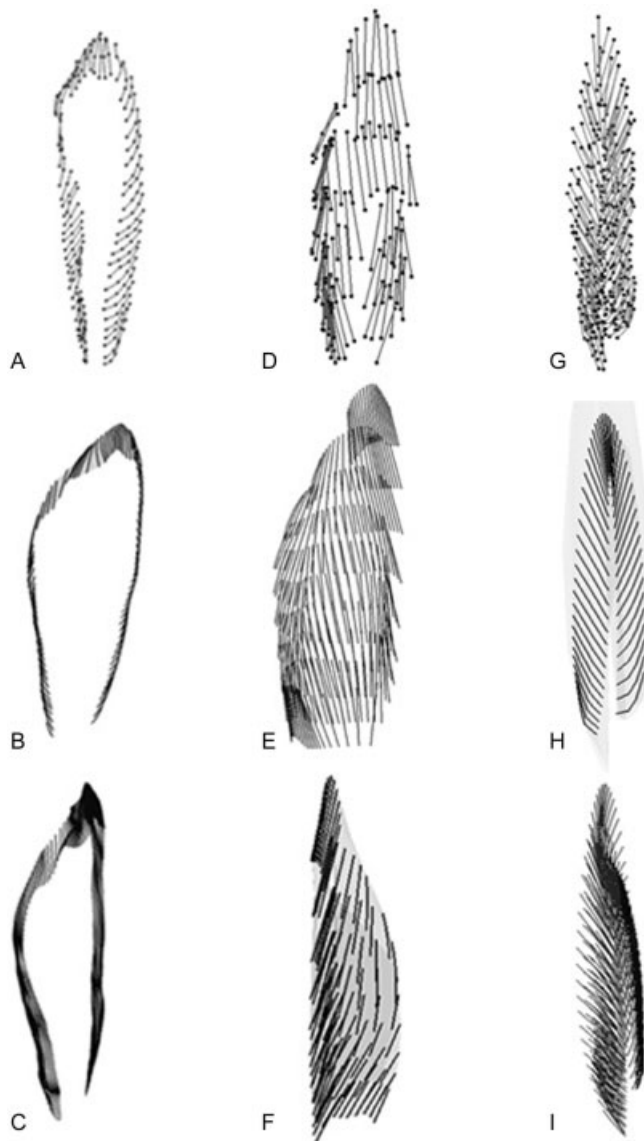


**Fig. 2.** 3D modelling of soleus muscle architecture. **A:** Marginal soleus (digitized data), posterior view. **B:** Marginal soleus (streamlines), posterior view. **C:** Marginal soleus (streamlines), posteromedial view. **D:** Posterior soleus (digitized data), posterior view. **E:** Posterior soleus (streamlines), posterior view. **F:** Posterior soleus (streamlines), anterolateral view. **G:** Anterior soleus (digitized data), posterior view. **H:** One layer of anterior soleus (streamlines), posterior view. **I:** Anterior soleus (streamlines), medial view.

lateral margins of the muscle, but are almost vertical proximally (Fig. 2A–C). The thin marginal soleus is modelled as one layer.

The posterior soleus consists of densely packed fiber bundles modeled in rows/columns. The fiber bundles pass from anterosuperiorly to posteroinferiorly (Fig. 2D–F).

The bipennate anterior soleus is modelled in layers (Fig. 2G,H). The original data set is based on four

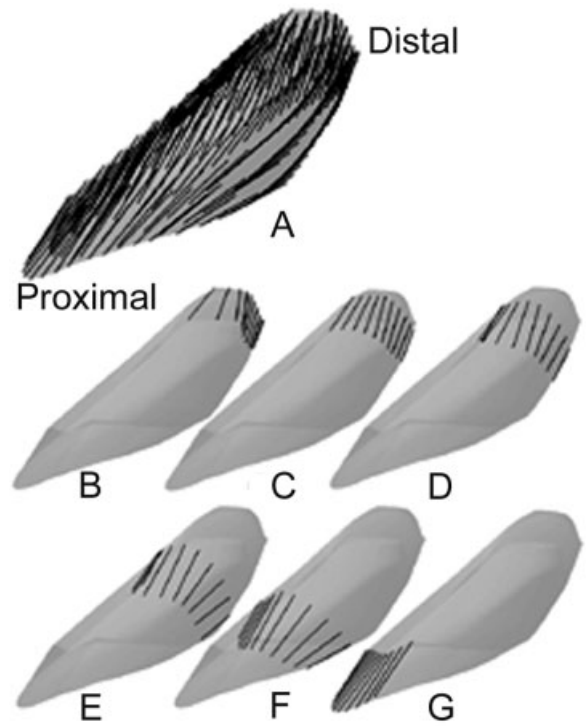


**Fig. 3.** Sequential arrangement of fiber bundles of posterior soleus. **A:** Posterior soleus, superomedial view. **B–G:** Sequential arrangement of fiber bundles from distal to proximal.

layers of serial dissection. Using the streamline function, new fiber bundles can be added to existing layers and to form new layer(s). The length of the anterior soleus, as a whole, increases from posterior to anterior when serially dissected (Fig. 2I).

**Documentation of Soleus Muscle Architecture**

The fiber bundle length and angles of pennation for the attachment sites of both ends of the fiber

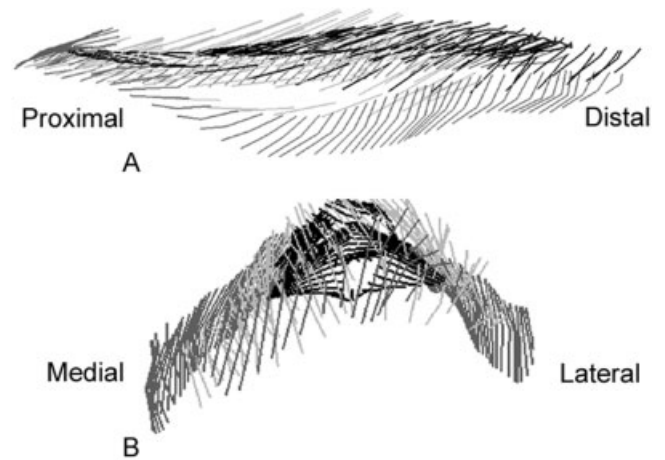


**Fig. 4.** Soleus: marginal (dark gray), posterior (light gray), and anterior (black). **A:** Superomedial view. **B:** Inferior view.

TABLE 2. Marginal Soleus

Marginal soleus	Average fiber bundle length <sup>a</sup>			“3D” angle of pennation <sup>b</sup>			
	Average FL ± SD (mm)	Range (mm)	Number of fiber bundles	Average AP ± SD (degrees)		Range (degrees)	
				θ <sub>A</sub>	θ <sub>P</sub>	θ <sub>A</sub>	θ <sub>P</sub>
Proximal 1/3							
Lateral	31.9 ± 2.4	27–36	22	52.5 ± 16.5	41.1 ± 19.9	36–88	22–88
Medial	33.7 ± 5.7	27–45	18	42.1 ± 23.3	32.4 ± 18.7	7–85	3–81
Middle 1/3							
Lateral	32.9 ± 3.3	29–39	16	48.7 ± 4.2	42.2 ± 5.3	43–59	36–55
Medial	32.3 ± 1.9	29–35	18	53.4 ± 8.7	40.4 ± 12.3	32–67	14–56
Distal 1/3							
Lateral	32.3 ± 2.9	27–38	11	59.6 ± 8.8	25.8 ± 11.2	48–73	7–45
Medial	29.6 ± 4.9	16–35	15	67.0 ± 11.3	20.9 ± 11.1	49–87	7–50

<sup>a</sup>Average fiber bundle length (FL) ± standard deviation (SD).

<sup>b</sup>3D angle of pennation (AP) ± standard deviation (SD) measured relative to the anterior aponeurosis (θ<sub>A</sub>) and posterior aponeurosis (θ<sub>P</sub>).

bundle were computed using the B-spline solid software. The computer modelling has allowed for measurement of the fiber length and pennation angles in 3D space throughout the volume of the marginal, posterior, and anterior soleus.

The average fiber bundle length of the different parts of marginal soleus was found to be between 30 and 34 mm, but it should be noted that the shortest fiber bundle was 16 mm and the longest 45 mm (Table 2). A trend of decreasing average fiber bundle length from proximal to distal was observed on the medial side of the marginal soleus. The anterior and posterior angle of pennation measurements were diverse, ranging from 3 to 88 degrees (Table 2). The average anterior angle of pennation was greater than the average posterior angle of pennation for all regions of marginal soleus.

The average fiber bundle length of the different parts of the posterior soleus ranged from 33 to 44 mm, with the shortest fiber bundle having a length of 31

mm and the longest 45 mm (Table 3). The middle (central) part of the proximal, middle, and distal thirds had the longest average fiber bundle length, followed by the lateral part. The medial part tended to have the shortest average fiber bundle length in all thirds of posterior soleus. The average anterior angle of pennation of the different parts was between 6 and 29 degrees (Table 3). The average posterior angle of pennation of the different parts was between 8 and 24 degrees. The anterior angle ranged from 1 to 35 degrees and the posterior angle from 4 to 30 degrees.

The average fiber bundle length of the parts of anterior soleus was between 30 and 40 mm with a range from 24 to 41 mm (Table 4). The shortest fiber bundles were located in the distal third. The proximal and middle thirds of the lateral side of the muscle had longer average fiber lengths than the medial side, indicating possible functional differences. The average angle of pennation relative to the median septum

TABLE 3. Posterior Soleus

Posterior soleus	Average fiber bundle length <sup>a</sup>			“3D” angle of pennation <sup>b</sup>			
	Average FL ± SD (mm)	Range (mm)	Number of fiber bundles	Average AP ± SD (degrees)		Range (degrees)	
				θ <sub>A</sub>	θ <sub>P</sub>	θ <sub>A</sub>	θ <sub>P</sub>
Proximal 1/3							
Lateral	40.3 ± 2.2	38–43	4	15.6 ± 0.9	17.7 ± 1.9	15–17	16–20
Middle	43.5 ± 1.1	42–45	6	7.5 ± 2.3	8.3 ± 4.2	5–12	4–15
Medial	38.4 ± 1.3	37–40	4	6.3 ± 6.2	11.0 ± 2.1	1–14	8–13
Middle 1/3							
Lateral	42.2 ± 1.2	41–44	7	13.2 ± 1.8	11.2 ± 2.7	12–17	7–15
Middle	42.5 ± 1.5	41–45	8	15.4 ± 7.5	17.5 ± 6.4	4–27	5–25
Medial	33.9 ± 2.2	31–38	8	16.7 ± 1.8	10.1 ± 2.6	14–18	6–13
Distal 1/3							
Lateral	37.8 ± 2.4	35–41	5	22.3 ± 6.6	21.9 ± 7.6	13–30	9–27
Middle	39.4 ± 1.3	38–41	4	29.1 ± 5.2	24.0 ± 5.0	24–35	18–30
Medial	32.9 ± 1.0	32–34	4	17.9 ± 2.6	7.9 ± 1.9	16–21	6–11

<sup>a</sup>Average fiber bundle length (FL) ± standard deviation (SD).

<sup>b</sup>3D angle of pennation (AP) ± standard deviation (SD) measured relative to the anterior aponeurosis (θ<sub>A</sub>) and posterior aponeurosis (θ<sub>P</sub>).

TABLE 4. Anterior Soleus

Anterior soleus	Average fiber bundle length <sup>a</sup>			"3D" angle of pennation <sup>b</sup>			
	Average FL $\pm$ SD (mm)	Range (mm)	Number of fiber bundles	Average AP $\pm$ SD (degrees)		Range (degrees)	
				$\theta_{AP}$	$\theta_{MS}$	$\theta_{AP}$	$\theta_{MS}$
Tip							
Lateral	36.6 $\pm$ 0.6	36–37	5	4.8 $\pm$ 4.3	6.6 $\pm$ 5.1	0.1–11	0.3–13
Medial	35.0 $\pm$ 0.7	34–36	5	1.0 $\pm$ 0.6	1.7 $\pm$ 1.1	0.1–2	0.3–3
Proximal 1/3							
Lateral	40.2 $\pm$ 1.3	38–41	9	32.2 $\pm$ 12.5	10.2 $\pm$ 6.4	15–51	0.1–19
Medial	32.7 $\pm$ 0.7	32–34	6	2.2 $\pm$ 1.3	3.2 $\pm$ 0.8	0.6–4	2–4
Middle 1/3							
Lateral	38.6 $\pm$ 1.9	36–41	5	5.8 $\pm$ 4.2	17.3 $\pm$ 2.8	3–13	13–20
Medial	32.3 $\pm$ 0.2	32–33	5	7.8 $\pm$ 4.5	1.8 $\pm$ 0.4	2–13	1–3
Distal 1/3							
Lateral	30.3 $\pm$ 3.1	26–34	5	6.5 $\pm$ 1.4	18.2 $\pm$ 3.7	4–8	12–21
Medial	29.6 $\pm$ 2.9	24–33	11	20.3 $\pm$ 3.8	15.6 $\pm$ 11.6	13–24	3–34

<sup>a</sup>Average fiber bundle length (FL)  $\pm$  standard deviation (SD).

<sup>b</sup>3D angle of pennation (AP)  $\pm$  standard deviation (SD) measured relative to the anterior aponeurosis ( $\theta_{AP}$ ) and median septum ( $\theta_{MS}$ ).

was greater in the lateral side of the muscle in all regions studied (Table 4).

## DISCUSSION

### Visualization of Muscle Architecture Using a B-Spline Solid Model

To date, no study has documented muscle architecture throughout the volume of a muscle. Visualization of muscle architecture has been limited to 2D planes using sectioned cadaveric muscle (Trzenschik and Loetzke, 1969; Wickiewicz et al., 1983; Friederich and Brand, 1990) or in vivo ultrasound (Kawakami et al., 1998; Maganaris et al., 1998; Chow et al., 2000; Martin et al., 2001). Anatomical photogrammetry, in conjunction with B-spline modelling, has enabled the creation of a 3D manipulatable model of an entire soleus muscle from one cadaver. The soleus muscle can be viewed in its entirety, as marginal, anterior, and posterior parts, or as individual rows/layers of fiber bundles within the marginal, anterior, and posterior parts. One of the advantages of using B-spline modelling is that it can mathematically interpolate the original data set (template) to create any number of fiber bundles (streamlines). This feature enables viewing of the fiber architecture at various levels of complexity.

The model is designed to permit the addition of connective tissue elements, such as aponeuroses, septa and tendons, and the underlying bony skeleton, including the ankle (talocrural) joint. It is hoped that in subsequent studies these data will be collected in addition to the fiber bundle data.

### Measurement of Architectural Parameters of Human Muscle

The plane of section of the cadaveric muscle must be such that the fiber bundles can be seen in their entirety between attachment sites. In previous studies, fiber bundle length has been measured manually from cadaveric tissue using a ruler or calipers (Trzenschik and Loetzke, 1969; Wickiewicz et al., 1983; Friederich and Brand, 1990).

Similarly, the angle of pennation has been measured using a protractor. This method results in a 2D conceptualization of muscle; however, muscle is a 3D structure that can have a complex fiber arrangement. If a 2D pennation angle is used to calculate the muscle force, it would only be computing the force magnitude projected onto the measuring plane. The other component of the force would not be calculated, but ignored. Furthermore, the locations of the measured fiber bundles are often not specifically stated, leading to difficulties in the interpretation of results.

The length and the two angles of pennation (at the attachment site of each end of the fiber bundle) can be measured in 3D space using the B-spline model. Large numbers of streamlines can be quantified using the fiber bundles of the original template.

By definition, the angle of pennation is the angle at which the muscle fibers are oriented to the line of force generation of a muscle (Trzenschik and Loetzke, 1969; Wickiewicz et al., 1983; Friederich and Brand, 1990). Wickiewicz et al. (1983) estimated a line of force and approximated the angles relative to that line using a protractor. When measuring pennation angle in complex muscles, such as the soleus, the angle is usually measured relative to the aponeurotic

attachment of the fiber bundle (Trzenschik and Loetzke, 1969; Alexander and Vernon, 1975; Maganaris et al., 1998). Measuring the angle of pennation relative to a single line of action for the entire posterior soleus would be difficult due to the size and shape of the muscle. Furthermore, in studies that have measured the angle of pennation relative to an estimated line of force, it is not clear where the line was located or how the estimation was made (Wickiewicz et al., 1983; Spoor et al., 1991).

In this study, the angle of pennation is the angle between the tangent vector of the fiber bundle and the tangent plane of the muscle surface at the point where the fiber bundle meets the aponeurosis. Traditionally, a fiber bundle is traced to its attachment on the aponeurosis, the protractor is aligned with the aponeurosis, and the angle to the fiber bundle measured in 2D. Although visualization and calculation of structural parameters in three dimensions is standard practice in other disciplines, this has not been the case with human or animal muscle. Muscle models reported in the literature are generally linear and unable to incorporate complex muscle architecture and 3D data. Musculoskeletal software systems have modelled muscles as a single force vector, that is, by one straight line or a series of line segments connected together (Delp and Loan, 1995). The direction of the force vector is determined by the muscle architecture. The muscle architecture is often based on the PCSA (physiological cross sectional area) formula, which includes only one average angle of pennation and one average fiber length for an entire muscle, neglecting the fact that pennation and fiber length can vary non-uniformly throughout a multi-part muscle. This representation also fails to account for moments that are exerted about the line of action, especially in complex muscles with large attachment sites (Van der Helm and Veenbaas, 1991).

Past analyses have used cross sectional area calculations based on muscle thickness (Ichinose et al., 1998); others have used PCSA incorporating angle of pennation and fiber length (Wickiewicz et al., 1983). Brand et al. (1986) concluded that it is not possible to predict which one of the three specimens they studied would generate the most force based on PCSA. Fukunaga et al. (1996) presented data that "suggest that factors other than PCSA contribute to the force output potential of plantar flexors and dorsiflexors in humans."

The use of a single line of action and the assumption that the fiber bundle length and angle of pennation is uniform throughout a muscle is common in modelling studies, including the soleus (White et al., 1984; Legreneur et al., 1996; Legreneur et al., 1997).

In reality, muscle architecture is complex, but now, with the aid of computer technology, it is possible to study muscle architecture in detail. Interaction between the contractile and connective tissue elements likely results in complex transmission and summation of forces. Continued development of the B-spline model to include connective tissue elements and bone may provide a new 3D approach to viewing and understanding skeletal muscle.

### **Fiber Bundle Length and Angle of Pennation of Cadaveric Human Soleus Muscle**

Haines (1932), Wickiewicz et al. (1983), and Friedrich and Brand (1990) reported a single measurement of average fiber length for the entire soleus ranging from 19.5 to 34.0 mm. The posterior and anterior soleus were documented separately by Trzenschik and Loetzke (1969) and Spoor et al. (1991); the posterior soleus as a whole was found to have an average fiber length of 28.6 and 25.8 mm, respectively. In the muscle used in this modelling study, the posterior soleus was divided into nine parts with the average fiber length ranging from 32.9 to 43.5 mm. The middle fiber bundles throughout the posterior soleus had the longest average fiber bundle lengths. In our study, the anterior soleus was divided into eight parts. The average fiber bundle length ranged from 29.6 to 40.2 mm, with the lateral side having a longer average fiber length than the medial side. For anterior soleus, Spoor et al. (1991) reported an average fiber bundle length of 26.7 mm and Trzenschik and Loetzke (1969) an average fiber bundle length of 27.8 mm. In this study, the architectural variability within the posterior and anterior soleus is evident with a 10.6 mm difference between the shortest and longest average fiber bundle length in both anterior and posterior soleus. The marginal soleus has not been previously studied. The fiber bundles of marginal soleus, connecting the edges of the posterior aponeurosis to the anterior aponeurosis and to the tibia and fibula, were found to have an average fiber bundle length of 29.6 to 33.7 mm. The average fiber bundle length tended to decrease from proximal to distal, most noticeably along the medial aspect.

The B-spline model of the soleus dissected in situ had longer average fiber bundle lengths for all the regions than the previous studies. This may be because the modelling results are based on one large specimen thus reducing the effect of variability between specimens. The average fiber bundle length could also be longer because the arc length of the fiber bundle is captured using the B-spline solid model. The length as measured in this study is based not only on the endpoints of attachment sites but also includes

intermediate points, therefore taking into account any curvature of the fiber bundle.

The “3D” angles of pennation obtained from the computer model cannot easily be compared to the traditional data. The distribution and extent of variation of the angle of pennation within the parts of soleus have not been previously documented. For example, in the marginal and anterior soleus, some fiber bundles were close to being horizontal whereas others were almost vertical.

### Functional Considerations

Some of the possible functional aspects of the soleus are discussed relative to the data obtained in the present study. The human soleus muscle has been described as an ankle plantar flexor and an important anti-gravity muscle for the maintenance of balance when standing (Campbell et al., 1973; Williams et al., 1989; Sinnatamby, 1999). The marginal, posterior, and anterior soleus, on contraction, may interact through their aponeuroses to contribute to these important functions.

The marginal soleus lies around the periphery of the muscle and is attached to both the anterior and posterior aponeuroses medially and laterally, but proximally lies between the posterior aponeurosis and the tibia and fibula. The marginal fiber bundles are curved, except where they attach to the proximal aspect of the tibia and fibula. In our pilot ultrasonographic studies, it was observed that when the marginal soleus contracted, the distance between the tibia and posterior aponeurosis decreased. This suggests that contraction of the fiber bundles of the marginal soleus tightened the posterior aponeurosis. Similarly, the marginal soleus, where it extends between the anterior and posterior aponeurosis may, on contraction, tighten both of these connective tissue sheaths. This action may take up the slack in the aponeuroses and maximize the efficiency of contraction of the posterior soleus.

The fiber bundles of posterior soleus form most of the volume of the muscle and are arranged obliquely between the anterior and posterior aponeuroses. Its posterior part is characterized by a large number of short fiber bundles packed into the muscle volume at relatively high angles of pennation. This makes the muscle ideal for generating high forces with little excursion (Lieber and Friden, 2000).

The anterior soleus, due to its attachment to the median septum and bipennate structure, can potentially play a role in ankle plantar flexion. Campbell et al. (1973) in an electromyographic study suggested that the medial and lateral aspects of soleus differ functionally with the lateral aspect being a stabilizer

of the leg and the medial aspect being an ankle plantar flexor. In this study we found that the lateral side of the posterior soleus had longer average fiber bundle lengths than the medial side, supporting the concept of a functional difference. However, from our results the lateral part having a longer fiber bundle length may have more of a role in ankle plantar flexion, and the medial part with a shorter fiber bundle length may be a better stabilizer. Campbell et al. (1973) used surface electrodes on the medial and lateral parts of soleus not concealed by gastrocnemius. The anterior soleus is more easily accessed from the medial side of the leg and it is possible that in Campbell et al. (1973) some of the signal came from the anterior soleus suggesting plantar flexion activity. The large number of veins traversing the soleus limits use of needle electrodes.

The human soleus muscle is a complex muscle with little known about how the marginal, anterior, and posterior parts interact and what their functional roles may be. “An understanding of the force transmission paths is tantamount to developing adequate models of structure-function relationships in skeletal muscle. It also permits more sophisticated interpretation of the functional effects of injury” (Patel and Lieber, 1997). Further work with a contractile B-spline model based on relaxed and contracted *in vivo* ultrasound data (Chow et al., 2000) may provide some answers to these questions.

### ACKNOWLEDGMENTS

We thank V. Oxorn for drawing Figure 1.

### REFERENCES

- Agur A, McKee N. 1997. Soleus muscle: fiber orientation. *Clin Anat* 10:130.
- Agur AM. 2001. Architecture of the human soleus muscle: three-dimensional computer modelling of cadaveric muscle and ultrasonographic documentation *in vivo*. University of Toronto, Toronto: Institute of Medical Science. 197 p.
- Alexander RM, Vernon A. 1975. The dimensions of knee and ankle muscles and the forces they exert. *J Human Movement Studies* 1:115–123.
- Ball KA, Pierrynowski MR. 1995. Estimation of six degree of freedom rigid body segment motion from two dimensional image data. *Human Movement Science* 14:139–154.
- Brand RA, Pedersen DR, Friederich JA. 1986. The sensitivity of muscle force predictions to changes in physiologic cross-sectional area. *J Biomech* 19:589–596.
- Campbell KM, Biggs NL, Blanton PL, Lehr RP. 1973. Electromyographic investigation of the relative activity among four components of the triceps surae. *Am J Phys Med* 52:30–41.

- Chow RS, Medri MK, Martin DC, Leekam RN, Agur AM, McKee NH. 2000. Sonographic studies of human soleus and gastrocnemius muscle architecture: gender variability. *Eur J Appl Physiol* 82:236–244.
- Delp SL, Loan JP. 1995. A graphics-based software system to develop and analyze models of musculoskeletal structures. *Comput Biol Med* 25:21–34.
- Enoka RM. 1988. Neuromechanical basis of kinesiology. Champaign, Illinois: Human Kinetics Books. p 155–181.
- Friederich JA, Brand RA. 1990. Muscle fiber architecture in the human lower limb. *J Biomech* 23:91–95.
- Fukunaga T, Ito M, Ichinose Y, Kuno S, Kawakami Y, Fukashiro S. 1996. Tendinous movement of a human muscle during voluntary contractions determined by real-time ultrasonography. *J Appl Physiol* 81:1430–1433.
- Haines RW. 1932. The laws of muscle and tendon growth. *J Anat* 66:578–585.
- Herzog W, ter Keurs HEDJ. 1988. A method for the determination of the force-length relation of selected in-vivo human skeletal muscles. *Pflügers Arch* 411:637–641.
- Huijing PA, van Lookeren Campagne AAH, Koper JF. 1989. Muscle architecture and fibre characteristics of rat gastrocnemius and semimembranosus muscles during isometric contractions. *Acta Anat* 135:46–52.
- Huijing PA, Woittiez RD. 1984. The effect of architecture on skeletal muscle performance: A simple planimetric model. *Neth J Zool* 34:21–32.
- Ichinose Y, Kanehisa H, Ito M, Kawakami Y, Fukunaga T. 1998. Morphological and functional differences in the elbow extensor muscle between highly trained male and female athletes. *Eur J Appl Physiol* 78:109–114.
- Kawakami Y, Ichinose Y, Fukunaga T. 1998. Architectural and functional features of human triceps surae muscles during contraction. *J Appl Physiol* 85:398–404.
- Legreneur P, Morlon B, Van Hoecke J. 1996. Simulation of in situ soleus isometric force output as a function of neural excitation. *J Biomech* 29:1455–1462.
- Legreneur P, Morlon B, Van Hoecke J. 1997. Joined effects of pennation angle and tendon compliance on fibre length in isometric contractions: a simulation study. *Arch Physiol Biochem* 105:450–455.
- Lieber RL, Friden J. 2000. Functional and clinical significance of skeletal muscle architecture. *Muscle Nerve* 23:1647–1666.
- Maganaris CN, Baltzopoulos V, Sargeant AJ. 1998. In vivo measurements of the triceps surae complex architecture in man: implications for muscle function. *J Physiol (Lond)* 512:603–614.
- Martin DC, Medri MK, Chow RS, Oxorn V, Leekam RN, Agur AM, McKee NH. 2001. Comparing human skeletal muscle architectural parameters of cadavers with in vivo ultrasonographic measurements. *J Anat* 199:429–434.
- Muhl ZF. 1982. Active length-tension relation and the effect of muscle pinnation on fiber lengthening. *J Morphol* 173:285–292.
- Ng-Thow-Hing V. 2001. Anatomically based models for physical and geometric reconstruction of humans and other animals. Toronto: Department of Computer Science. Toronto: University of Toronto. 162 p.
- Otten E. 1988. Concepts and models of functional architecture in skeletal muscle. *Exerc Sport Sci Rev* 16:89–139.
- Oxorn VM, Agur AM, McKee NH. 1998. Resolving discrepancies in image research: the importance of direct observation in the illustration of the human soleus muscle. *J Biocommun* 25:16–26.
- Patel TJ, Lieber RL. 1997. Force transmission in skeletal muscle: from actomyosin to external tendons. *Exerc Sport Sci Rev* 25:321–363.
- Pierrynowski MR. 1982. A physiological model for the solution of individual muscle forces during normal human walking. Department of Kinesiology. Burnaby, Canada: Simon Fraser University. 179 p.
- Pierrynowski MR, Morrison JB. 1985. A physiological model for the evaluation of muscular forces in human locomotion: theoretical aspects. *Math Biosci* 75:69–101.
- Press HP, Teukolsky SA, Vetterling WT, Flannery BP. 1992. Numerical recipes in C: the art of scientific computing. 2nd Ed. Cambridge: Cambridge University Press. 994 p.
- Roy RR, Ishihara A. 1997. Overview: Functional implications of the design of skeletal muscles. *Acta Anat* 159:75–77.
- Sinnatamby CS. 1999. Last's anatomy regional and applied. 10th Ed. London: Churchill Livingstone. p 141–142.
- Spoor CW, van Leeuwen JL, van der Meulen WJTM, Huson A. 1991. Active force-length relationship of human lower-leg muscles estimated from morphological data: a comparison of geometric muscle models. *Eur J Morphol* 29:137–160.
- Trzenschik K, Loetzke H-H. 1969. Strukturanalytische Untersuchungen am M. soleus des Menschen. *Anat Anz Bd* 124: 297–313.
- Van der Helm FCT, Veenbaas R. 1991. Modelling the mechanical effect of muscles with large attachment sites: application to the shoulder mechanism. *J Biomech* 24:1151–1163.
- van der Linden BJJJ, Koopman HFJM, Grootenboer HJ, Huijing PA. 1998. Modelling functional effects of muscle geometry. *J Electromyogr Kinesiol* 8:101–109.
- White SC, Yack HJ, Winter DA. 1984. A three-dimensional musculoskeletal model for gait analysis: anatomical variability estimates. *J Biomech* 22:885–893.
- Wickiewicz TL, Edgerton VR, Roy RR, Perrine J, Powell P. 1982. Human leg muscle architecture and force-velocity properties. *Med Sci Sports Exerc* 14:144.
- Wickiewicz TL, Roy RR, Powell PL, Edgerton VR. 1983. Muscle architecture of the human lower limb. *Clin Orthop* 179:275–283.
- Williams PL, Warwick R, Dyson M, Bannister LH, editors. 1989. Gray's anatomy. 37th Ed. London: Churchill Livingstone. p 647–648.
- Woittiez RD, Huijing PA, Boom HBK, Rozendal RH. 1984. A three-dimensional muscle model: a quantified relation between form and function of skeletal muscles. *J Morphol* 182:95–113.
- Woittiez RD, Huijing PA, Rozendal RH. 1983. Influence of muscle architecture on the length-force diagram of mammalian muscle. *Pflügers Arch* 399:275–279.
- Yamaguchi GT, Sawa AGU, Moran DW, Fessler MJ, Winters JM. 1990. A survey of human musculotendon actuator parameters. In: Winters JM, Woo SL-Y, editors. Multiple muscle systems. New York: Springer-Verlag. p 717–747.
- Zajac FE. 1989. Muscle and tendon: Properties, models, scaling, and application to biomechanics and motor control. *Crit Rev Biomed Eng* 17:359–411.